



## On the surface chemistry and the reuse of sulfur-doped TiO<sub>2</sub> films as photocatalysts

Rodrigo T. Bento<sup>a,b</sup>, Olandir V. Correa<sup>a</sup>, Marina F. Pillis<sup>a,\*</sup>

<sup>a</sup> Nuclear and Energy Research Institute, IPEN-CNEN/SP, University of São Paulo, Prof. Lineu Prestes Avenue, 2242, Brazil

<sup>b</sup> Universidade São Judas Tadeu, Taquari Street, 546, São Paulo, Brazil

### HIGHLIGHTS

- S-TiO<sub>2</sub> catalysts obtained under H<sub>2</sub>S atmosphere at low temperature are highly efficient.
- SO<sub>4</sub><sup>2-</sup> was formed on the films surface, indicating the substitution of Ti<sup>4+</sup> by S<sup>6+</sup>.
- XPS depth profile revealed the cationic diffusion of sulfur by the alternative S-doped method.
- S-doped TiO<sub>2</sub> film presented 72.1% of dye degradation under visible light.
- S-TiO<sub>2</sub> films exhibit high stability and efficiency around 70% in the first 3 cycles.

### ARTICLE INFO

#### Keywords:

Titanium dioxide  
Sulfur-doped TiO<sub>2</sub>  
MOCVD  
Recyclability  
Surface analysis

### ABSTRACT

The surface chemistry and recyclability of sulfur-doped titanium dioxide (TiO<sub>2</sub>) films was evaluated. The photocatalysts were grown by metalorganic chemical vapor deposition (MOCVD) at 400 °C. The films were sulfur-doped at 50 °C by using hydrogen sulfide (H<sub>2</sub>S) as sulfur source. The photocatalytic behavior of the films was measure by monitoring the methyl orange dye decolorization under visible light for several cycles. The films are formed only for the anatase crystalline phase. The results demonstrated that no structural modifications or significant differences in the morphology of the films occurred after their use. The sulfur-doped TiO<sub>2</sub> films presented good photocatalytic activity, with an efficiency of 72.1% under visible light in its first use. The durability experiments suggest that even with the dye impregnation on the catalyst surface, the photocatalytic activity of the S-doped TiO<sub>2</sub> films remained around 70% in the first 3 cycles, which allows their practical application for water treatment and purification under sunlight.

### 1. Introduction

Heterogeneous photocatalysis is a green advanced oxidative process (AOP) used as an alternative method for industrial wastewater treatment and environmental decontamination [1]. This method is based on the formation of hydroxyl radicals (HO•) from the use of a semiconductor material activated by solar radiation [2]. Although considerable papers have already been published concerning on the use of semiconductors as catalysts, there is still little data on their use as a supported film – which would facilitate material handling, surface reusability and subsequent reuse [3]. The possibility on the reuse of catalyst materials is an important differential feature, and it is necessary for efficient practical applications of heterogeneous photocatalysis in

water treatment.

Several problems may occur during the photocatalytic process especially when a suspension is used [4]. Catalyst separation from suspensions is a difficult and costly process. Furthermore, suspended particles tend to aggregate, especially at high concentrations. Thus, studies on the use of titanium dioxide (TiO<sub>2</sub>) films have been developed to improve the catalyst recovery and obtain better photocatalytic performance [5–7].

TiO<sub>2</sub> films have been widely investigated as a promising photocatalyst for the removal of organic contaminants from water and air [8]. The surface properties and crystalline structure of the semiconductor photocatalysts have great influence on the photocatalytic properties [9, 10]. Both anatase and rutile phases present photoactivity. Nevertheless,

\* Corresponding author.

E-mail address: [mfpillis@ipen.br](mailto:mfpillis@ipen.br) (M.F. Pillis).

<https://doi.org/10.1016/j.matchemphys.2021.124231>

Received 6 August 2020; Received in revised form 24 November 2020; Accepted 2 January 2021

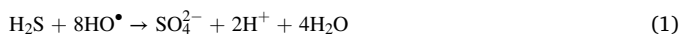
Available online 7 January 2021

0254-0584/© 2021 Elsevier B.V. All rights reserved.

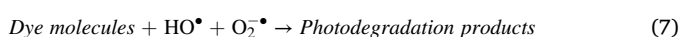
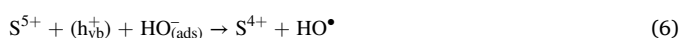
anatase-TiO<sub>2</sub> is the most efficient due to the high electron mobility, and greater surface area [11]. TiO<sub>2</sub> films can be obtained by different methods, among which the sol-gel [12] and chemical vapor deposition (CVD) [4,6,8]. CVD technique present important advantages, such as high deposition rate, well-defined stoichiometry, and the capacity to efficiently coat complex geometry surfaces [13], which promotes the synthesis of homogeneous films, an important attribute for the practical application of such catalysts.

However, the anatase-TiO<sub>2</sub> photoactivity is limited to the ultraviolet light (UV). The structural and surface modification of supported TiO<sub>2</sub> catalysts by the metallic or non-metallic ions doping process aims to improve their efficiency [5,14]. Among the chemical elements used as dopants, nitrogen and carbon are the most studied. Nevertheless, researches directed at sulfur (S) doping of TiO<sub>2</sub> have shown good results in environmental applications [15–17]. Han et al. [15], Ohno et al. [18], and Bayati et al. [19] studied the synthesis of sulfur-doped TiO<sub>2</sub>. The authors observed that S<sup>6+</sup> cation replace Ti<sup>4+</sup> ions into TiO<sub>2</sub> lattice, and this effect is more pronounced than the S<sup>2-</sup> anion-doped for visible-light photocatalytic activity. However, S-doped TiO<sub>2</sub> photocatalysts are usually obtained at temperatures above 300 °C [12,15].

The possibility of using hydrogen sulfide (H<sub>2</sub>S) as a sulfur precursor for low-temperature TiO<sub>2</sub> doping has recently been demonstrated. H<sub>2</sub>S is an odorous, toxic and corrosive compound, released as by-product of many industrial processes. Frequently TiO<sub>2</sub> is used for the gaseous decomposition of these released products at atmospheric pressure, between 20 °C and 150 °C, without the need of other chemicals, sulfur doping and surface modification of TiO<sub>2</sub> occurs directly [20,21] – which characterizes this novel technique as a green and low cost method. In our previous study [7], we showed that films of 350 nm-thick TiO<sub>2</sub> films S-doped at 50 °C using a H<sub>2</sub>/H<sub>2</sub>S gas mixture exhibited 38% of dye decolorization efficiency under visible light. However, the film thickness has a great influence on the photocatalytic behavior. Marcello et al. [22] showed that undoped TiO<sub>2</sub> films present a thickness ideal value for photocatalytic application on water treatment. Thus, 470 nm-thick TiO<sub>2</sub> photocatalysts were S-doped under H<sub>2</sub>/H<sub>2</sub>S mixture at 50, 100 and 150 °C [21]. The decomposition and adsorption of H<sub>2</sub>S on the TiO<sub>2</sub> surface at low temperature occurs due to the presence of HO• radicals, according to Eq. (1) [7], which oxidize sulfur and, consequently, promotes the formation of sulfate groups (SO<sub>4</sub><sup>2-</sup>) on the film surface, and Ti–O–S bonds in the semiconductor structure [7,20,23].



The results showed that the undoped anatase-TiO<sub>2</sub> film presents photoactivity only under exposure to UV radiation. S-doping process enabled TiO<sub>2</sub> activation under visible light, and the S–TiO<sub>2</sub> film doped at 50 °C exhibited the best photocatalytic activity, with photocatalytic efficiency around 72% of methyl orange dye decolorization [21]. The heterogeneous photocatalysis mechanism for using sulfated TiO<sub>2</sub> films, as proposed by the Lin et al. [24], follows the steps described by the following equations:



Nevertheless, studies aimed to the reusability and practical reuse of sulfated photocatalysts are still little approached in the literature, and the effects on the surface after several photocatalytic cycles under visible light were not discussed. Here, the possibility of reusing S-doped TiO<sub>2</sub> films on methyl orange dye removal process in the water under visible

light was evaluated. The catalysts were obtained by the metalorganic chemical vapor deposition (MOCVD) method, and subsequently sulfur doped at 50 °C under H<sub>2</sub>/H<sub>2</sub>S atmosphere.

## 2. Experimental

### 2.1. Synthesis of sulfur-doped catalysts

470 nm-thick TiO<sub>2</sub> catalysts were grown by MOCVD in the equipment previously described by Bento and Pillis [1]. The growth of the films was carried out on borosilicate glass substrates (25 × 76 × 1 mm) at 400 °C under a pressure of 50 mbar. Titanium (IV) isopropoxide (Sigma-Aldrich Co., purity 99,999%) was used as the titanium and oxygen sources, and N<sub>2</sub> was used as the carrier and the purge gas. Then, the catalysts were sulfur-doped by a facile thermochemical treatment previously described by Bento et al. [7]. The doping process were carried out at 50 °C for 60 min under a mixture of H<sub>2</sub>-2v.% H<sub>2</sub>S.

### 2.2. Characterization techniques

The catalysts were analyzed before and after use by X-ray diffraction (XRD) (Rigaku Multiflex, monochromatized CuKα radiation, incidence angle of 5°, scan rate of 0.02°, and with 2θ ranging from 5 to 80°), atomic force microscopy (AFM) on the tapping mode (SPM Bruker NanoScope IIIA, scan frequency of 0.601 Hz and in the area of 2 μm × 2 μm), X-ray photoelectron spectroscopy (XPS) (Thermo Scientific K-Alpha, with resolution of 0.1 eV, and spot size beam of 400 μm), contact angle measurements (SEO Phoenix-i, under visible light, dropping 5 μL of deionized water on the film surface for three times for each measurement; prior to the tests the films were stored for 120 h in a dark chamber to avoid the light interference, and Fourier Transform infrared (FTIR) (Thermo Nicolet spectrometer Nexus 870 FT-IR, in the frequency range of 500 cm<sup>-1</sup> to 2500 cm<sup>-1</sup> at 25°). Raman spectroscopy (WITEC Raman Microscope Alpha 300 R, exposure time of 30 s, λ = 532 nm, range of 0–1200 cm<sup>-1</sup>) was used to observe the structural properties of the sulfur-doped films unused and after 12 photocatalytic cycles. Before the analysis, the surface of the films was cleaned with ethyl alcohol [22,25].

### 2.3. Surface reusability and durability of the catalysts

The durability of the S-doped TiO<sub>2</sub> films were evaluated by the dye decolorization after several photocatalytic cycles under visible light (Royal Philips Electronics; four tubular LED lamps with 3 W each; λ = 400–700 nm). Each cycle consists of 5 h of test, and the degradation measurements are taken every 60 min. The photocatalytic experiments were realized in a homemade visible-light reactor setup previously described [1]. Methyl orange dye was used as pollutant model (0.005 g L<sup>-1</sup>), at pH = 2, and volume of 40 mL. The initial dye concentration, pH of the reaction medium, and solution volume were the same as those used in studies previously developed by the group [7,22]. Changes in dye concentration were accompanied by UV–Vis spectroscopy (Global Trade Technology), through the characteristic peak of the chromophore group at λ = 464 nm. S–TiO<sub>2</sub> film and dye solution remained into the dark for 1 h to achieve the adsorption-desorption equilibrium of the dye molecules on the photocatalyst surface [22]. The experiments were kept under controlled temperature in the range of 19–20 °C. For catalyst reusability, at the end of each photocatalytic cycle, the films were individually washed with ethanol for 10 min, rinsed with deionized water and dried with N<sub>2</sub>. The respective reusability method was defined from previous studies [3,22,25].

## 3. Results and discussion

### 3.1. XPS results

XPS technique was employed to evaluate the chemical state of the

formed species near the S-doped catalyst surface. C1s peak at 284.8 eV was set as reference. Fig. 1a exhibits the XPS depth profile of the sulfur-doped TiO<sub>2</sub> film, demonstrating the chemical concentration as a function of sputter depth. The spectra showed the predominant presence of O and Ti on the surface. Carbon is also present in a significant amount and is attributed to adventitious carbon and to the residual carbon from the metalorganic precursor [26,27]. However, the C atomic percentage inside the film decreases considerably since the surface adventitious carbon is removed by the XPS sputtering for the depth profile analysis. In this way, the Ti:O ratio increases with the sputter time: from 1:3.45, on the S-TiO<sub>2</sub> film surface (higher carbon concentration), to 1:2.66, 1:2.43, 1:2.37, and 1:2.43, respectively, after 675, 945, 1215, and 1485 s of sputter time. Therefore, it was observed that the Ti:O ratio becomes constant inside the film, where there is only the presence of the residual carbon. The depth profile revealed the presence of sulfur, denoting the successful inclusion of S ions into the TiO<sub>2</sub> film, with a sulfur concentration around 8 at%.

Fig. 1b shows the high resolution S2p XPS spectrum. The results revealed the presence of S<sup>6+</sup> cations, possibly replacing the Ti<sup>4+</sup> ions [7, 16,18,28]. This behavior promotes the formation of SO<sub>4</sub><sup>2-</sup> groups on the TiO<sub>2</sub> surface, and Ti-O-S bonds into its structure [21,24]. No indication of S<sup>2-</sup> formation was observed at 161 eV, suggesting that it does not exist on the catalyst surface. Ohno et al. [29] and Umebayashi et al. [30] observed that the sulfur ionic radius (S<sup>2-</sup> - 0.174 nm) is greater than the oxygen ionic radius (O<sup>2-</sup> - 0.132 nm), which makes it difficult to replace the O<sup>2-</sup> by anions S<sup>2-</sup>. Several papers have been suggested the importance of S<sup>6+</sup> for S-doped catalysts [29–31]. The S cation substitution is chemically more favorable for environmental applications than the S anion substitution, due to the formation of centers for trapping electron (e<sup>-</sup>)/hole (h<sup>+</sup>) pairs, and consequent reduction of the electronic recombination rate [32,33]. It was also observed that the concentration of sulfur remains constant in the catalyst thickness, which confirms its diffusion, and suggests the uniform distribution in depth TiO<sub>2</sub>.

Fig. 2 shows the evolution of the high resolution XPS spectrum of S2p core-level region with the sputtering time for the S-doped TiO<sub>2</sub> film. It was clearly observed that S2p<sub>3/2</sub> signal is detected in the film surface even at the beginning of the experiment, until at the end of the depth profile experiment, and achieve the borosilicate glass substrate. The same component was founded when the spectrum was deconvoluted (Fig. 1b). The result suggests that the alternative S-doped method allowed the cationic diffusion of sulfur in the S<sup>6+</sup> chemical state, and the formation of superficial SO<sub>4</sub><sup>2-</sup> groups. The sulfur chemical state did not change in depth profile. The binding energy component at 169 eV shows good similarity to the literature [7,16,19,29]. No peaks at 167 eV and 162 eV were found, which can indicate the absent of sulfur oxidation in +4 or -2 chemical states, respectively.

### 3.2. Structural and morphological analysis of S-doped catalysts

The crystallinity and phases formed in the 470 nm-thick S-doped TiO<sub>2</sub> film grown at 400 °C, and submitted to several photocatalytic cycles, were investigated by XRD, according to Fig. 3. The phases formed

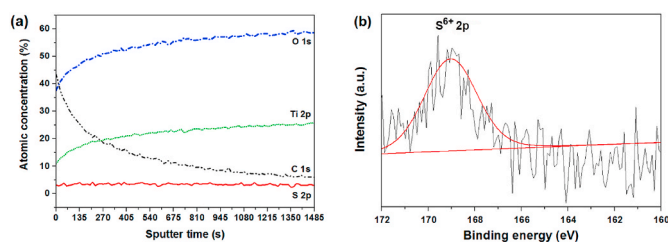


Fig. 1. (a) XPS sputter depth profile of the sulfur-doped TiO<sub>2</sub> film; (b) High resolution XPS spectrum of S2p region with the fitted curve of sulfur-doped catalyst.

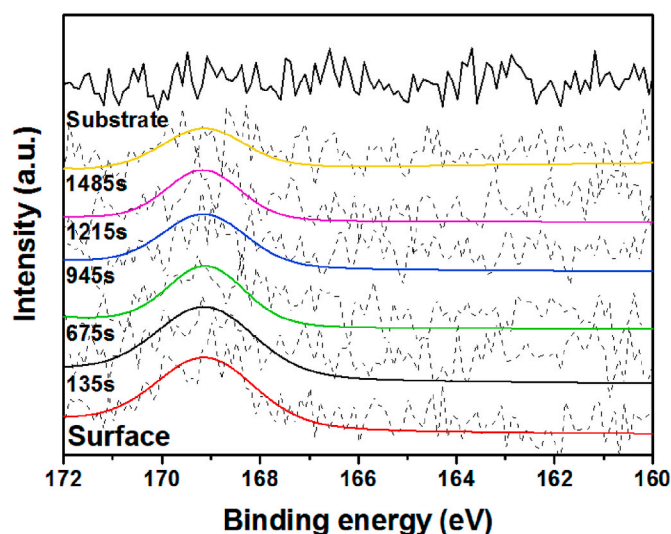


Fig. 2. Evolution of the high resolution XPS spectra of S2p region with the sputtering time for 470 nm-thick S-TiO<sub>2</sub> film doped with H<sub>2</sub>/H<sub>2</sub>S at 50 °C. The black dashed lines are the XPS spectra, and the colored continuous lines are the respective S2p core-level fitted curves for each sputtering time of the film depth profile: from the S-TiO<sub>2</sub> films surface to the borosilicate glass substrate.

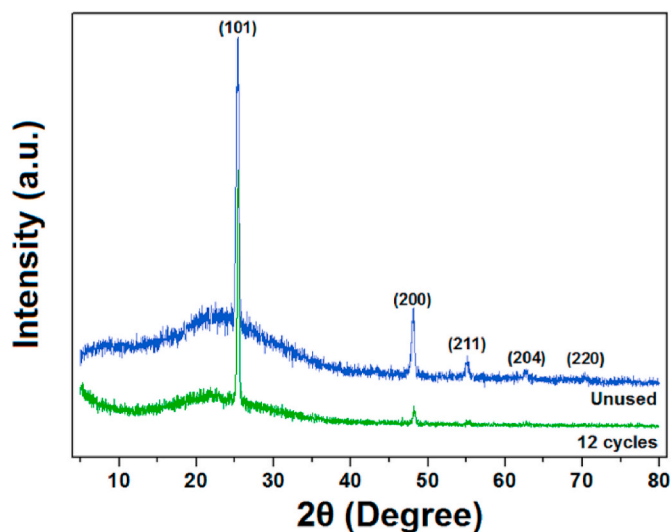
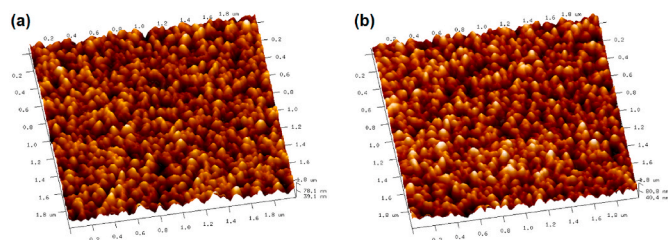


Fig. 3. XRD patterns of the sulfur-doped TiO<sub>2</sub> film, before and after its use in the methyl orange dye degradation experiments under visible light during 12 photocatalytic cycles. (For interpretation of the references to color in this figure legend, the reader is referred to the Web version of this article.)

were identified with the JCPDS (Joint Committee on Powder Diffraction Standards) database. The catalyst presented anatase-TiO<sub>2</sub> phase, according to the JCPDS 21-1272 and showed good crystallinity [2,7,15]. The results indicated that the S-doped TiO<sub>2</sub> film exhibited the same characteristic peaks after 12 photocatalytic cycles of 300 min each. Such behavior suggests that there was no change in the catalyst structure after the methyl orange dye degradation experiments or exposure to air, which indicates its good stability. No delamination was observed in the film after the tests, which is an important attribute for practical application.

Fig. 4 exhibits the surface images of S-doped TiO<sub>2</sub> film obtained by AFM. No significant differences in film morphology were observed before or after photocatalysis tests. The surface of the film presents small round grains due to the presence of SO<sub>4</sub><sup>2-</sup> groups formed on the catalyst surface after the low-temperature S-doping process [19,34]. Previous



**Fig. 4.** AFM 3D images of the sulfur-doped TiO<sub>2</sub> film: (a) unused catalyst surface; (b) catalyst surface after 12 photocatalytic cycles under visible light.

research paper demonstrated that the SO<sub>4</sub><sup>2-</sup> formation on TiO<sub>2</sub> surface, by the S-doped process with H<sub>2</sub>/H<sub>2</sub>S mixture at low temperature, promotes significant changes in morphological characteristics of the films – effect that favors its visible light photocatalytic application [7,20,28]. Table 1 shows the mean grain size and RMS (Root Mean Square) roughness values of the film before and after the degradation tests under visible light. Mean grain size analyses were performed using the ImageJ® image processing software, determined by Feret diameter of the particles. For the unused S-doped catalyst (Fig. 4a), the values found were 104 nm and 8.6 nm for mean grain size and roughness, respectively. After 12 photocatalytic cycles (Fig. 4b), the film exhibited a mean grain size of 112 nm and RMS roughness of 9.1 nm. Such values are favorable for photocatalytic applications, since contact of the adsorbed pollutant substance with the catalyst surface is facilitated, and consequently results in increased photocatalytic efficiency of the films [13, 35].

Surface wettability is an important morphological characteristic of supported catalysts for photocatalytic application. Fig. 5 presents the contact angle values for the drop profile formed on the S-doped catalyst surface before (Fig. 5a) and after 12 photocatalytic cycles under visible light (Fig. 5b). The results indicated the high hydrophilicity of the S-doped TiO<sub>2</sub> film grown by MOCVD, and sulfur-doped at low temperature under H<sub>2</sub>/H<sub>2</sub>S atmosphere. Such a hydrophilic character facilitates the transfer of electrons, and increases its photocatalytic activity [21,25, 36]. After the dye removal experiments, there was a slight loss of surface wettability. Nevertheless, the S-doped catalyst still retained its hydrophilic properties.

FTIR spectra of S-doped TiO<sub>2</sub> film before and after 12-cycle methyl orange dye photodegradation experiments are shown in Fig. 6. The unused catalyst presented a long absorption band in the 500–700 cm<sup>-1</sup> range, attributed to the symmetrical stretching vibration of the Ti–O bonds [37]. The band at 1630 cm<sup>-1</sup> refers to the hydroxyl groups adsorbed on the surface of the films. The two absorbance peaks around 1040 cm<sup>-1</sup> and 1135 cm<sup>-1</sup> indicate the presence of Ti–O–S bonds [15], which confirms the incorporation of S into the TiO<sub>2</sub> structure and corroborate the XPS results. The band at 1135 cm<sup>-1</sup> represents an S–O vibration, characteristic of the SO<sub>4</sub><sup>2-</sup> groups present on the catalyst surface. Nevertheless, after the photocatalytic tests were performed, it occurs a change in the FTIR spectrum profile of the S-doped film between 500 and 1625 cm<sup>-1</sup>. This result suggests that dye molecules impregnated the catalyst surface after its use. The bands observed at 562 cm<sup>-1</sup> and 575 cm<sup>-1</sup> correspond to the C–S stretching vibrations, suggesting the formation of new products from degradation process of sulfonated aromatic rings or benzene rings [38]. The C–H vibrations of

**Table 1**  
Morphological characteristics of low-temperature S-doped TiO<sub>2</sub> film before and after application over 12 photocatalytic cycles under visible light.

|                                 | Mean grain size (nm) | RMS roughness (nm) | Contact angle |
|---------------------------------|----------------------|--------------------|---------------|
| unused S-doped TiO <sub>2</sub> | 104                  | 8.6                | 12°           |
| After 12 photocatalytic cycles  | 112                  | 9.1                | 20°           |

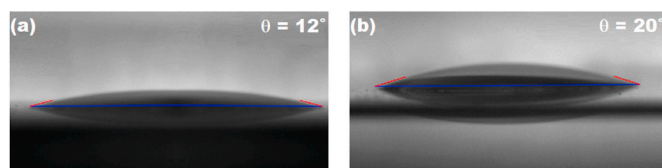


**Fig. 5.** Contact angle measurements for the deionized water drop profile (5 µL) on the surface of the sulfur-doped TiO<sub>2</sub> film: (a) unused catalyst; (b) after 12 photocatalytic cycles under visible light. Before to tests, the film was stored for 120 h in a dark chamber to avoid the light interference.

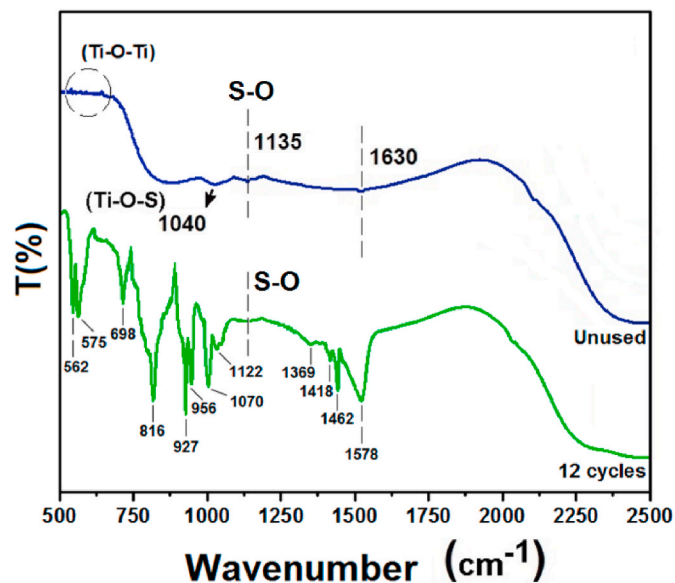


**Fig. 6.** FTIR spectra of the sulfur-doped TiO<sub>2</sub> film, before and after 12 photocatalytic cycles in the methyl orange dye degradation experiments under visible light. (For interpretation of the references to color in this figure legend, the reader is referred to the Web version of this article.)

the benzene ring are located at 698 cm<sup>-1</sup>, 816 cm<sup>-1</sup> and 956 cm<sup>-1</sup>. The two absorbance peaks around 1070 cm<sup>-1</sup> and 1122 cm<sup>-1</sup> refer to the S=O vibration [38]. The C–N stretching vibrations were assigned to the band at 1369 cm<sup>-1</sup>. The N=N vibration appears around 1418 cm<sup>-1</sup>. The bands at 1462 cm<sup>-1</sup> and 1578 cm<sup>-1</sup> indicate the C–C vibration of the benzene structure [39]. The peak of S–O bonds at 1135 cm<sup>-1</sup> can still be observed, which indicates that SO<sub>x</sub> groups remain present on the TiO<sub>2</sub> surface. Such behavior suggests a possible superficial saturation of the adsorption sites of the film, even after the catalyst reusability.

### 3.3. Photocatalytic behavior of S-doped TiO<sub>2</sub> films

The visible light wavelength corresponds to 45% of the total radiation energy from the Sun [40]. In this way, the photoactivation of TiO<sub>2</sub> catalysts in the visible region becomes a promising aspect, considering the optimization of solar radiation utilization, as well as allowing its practical application in indoor environments by the use of visible light lamps (λ = 400–700 nm) [7,15,25]. The photocatalytic behavior of the S-doped TiO<sub>2</sub> film was evaluated on the methyl orange dye decolorization under visible light. The durability of the catalyst was observed during its exposure to 12 photocatalytic cycles of 5 h each, under the same conditions, accounting for a total of 60 h of experiment. For the catalyst surface reusability, the S-doped film was washed with ethanol at the end of each cycle. Marcello et al. [22] evaluated the influence of different surface reusability methods on durability and recyclability of TiO<sub>2</sub> films. The authors used deionized water, ethanol, and acetone to clean the film surface. The results suggested that the surface reusability

method using ethanol promoted greater photocatalytic stability along several cycles. The use of ethanol to clean supported catalysts allows to partially remove the adsorbed dye on the film surface, which results in the maintenance of surface area and adsorption sites [3,22].

Considering the Beer-Lambert law [1,41], the photocatalytic efficiency of S-doped films ( $E_f$ ) can be calculated according to Eq (8):

$$E_f = \left( \frac{C_0 - C}{C_0} \right) \times 100\% \quad (8)$$

where  $C_0$  is the model pollutant initial concentration, and  $C$  is the concentration of the pollutant at time  $t$  of radiation and catalyst exposure. According to previous studies, undoped anatase-TiO<sub>2</sub> film do not present photocatalytic activity under visible light [7,25,42]. Fig. 7a exhibits the dye concentration variation over 12 photocatalytic cycles as a function of the time of exposition to S-doped catalyst under visible light. It is observed that the S-doped TiO<sub>2</sub> film presented an initial performance of 72.1% in 5 h of test. The photocatalytic activity of the film remained around 70% in the first 3 cycles, totaling 16 h of use with good removal behavior of the model pollutant. Such photocatalytic stability found in the process can be attributed to the non-significant alteration of catalyst structure and morphology, as observed in the characterization step. However, from the 4th reusability there was a loss of photoactivity, in which the S-doped catalyst exhibited a mean efficiency of 52.8% between the 4th and 6th photocatalytic cycle. The photocatalytic activity decreased slightly in the 7th and 8th cycles, where the dye photodegradation efficiencies obtained were 42.5% and 42.1%, respectively. Finally, between the 9th and 12th photocatalytic cycle, the photoactivity of the film stabilized at around 35%.

Fig. 7b shows the dye removal kinetic curves of S-TiO<sub>2</sub> film along the 12 photocatalytic cycles, in which it is possible to evaluate the apparent rate constant ( $k_{app}$ ) for methyl orange dye decolorization from the linear relationship  $\ln(C_0/C)$  and irradiation time [22]. Photodegradation kinetics follows the Langmuir-Hinshelwood model, according a pseudo-first order degradation for reactions where the pollutant concentration is very low [43,44]. The results demonstrated that throughout the first 6 photocatalytic cycles, the behavior of the S-doped catalyst at the beginning of the dye decolorization experiments (1 h) was similar, with  $k_{app}$  values around  $3.8 \times 10^{-4} \text{ h}^{-1}$ , as shown in Table 2. The main photocatalytic activity of TiO<sub>2</sub> films occurs in the first hour of testing. This effect is caused by adsorbates induced by rapid initial degradation, which may prevent further photocatalytic reactions [45]. The initial stage of the photocatalytic reaction by pseudo-first order kinetic mechanisms is the attack on the dye molecules by the HO• radicals. Along the decolorization process, the HO• generation remains constant, and it reacts only with the organic pollutant [44].

From the 7th photocatalytic activation cycle there is a slight decrease

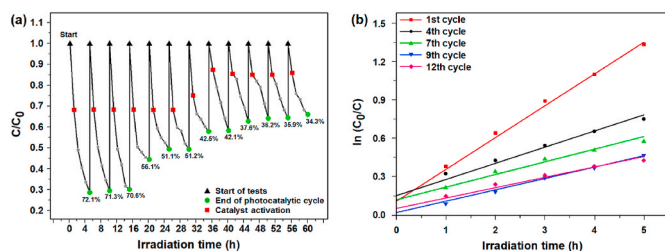


**Fig. 7.** (a) Photocatalytic efficiency of the sulfur-doped TiO<sub>2</sub> film during 12 cycles, with a total of 60 h of experiment under visible light. The film was grown on borosilicate glass substrates at 400 °C by MOCVD method, and then sulfur-doped at low temperature under H<sub>2</sub>/H<sub>2</sub>S atmosphere. The behavior of the catalysts was observed in the methyl orange dye degradation: concentration of 5 mg L<sup>-1</sup>, pH = 2, and volume of 40 mL. (b) Pseudo-first order kinetic curves of S-TiO<sub>2</sub> film for dye removal under visible light. (For interpretation of the references to color in this figure legend, the reader is referred to the Web version of this article.)

**Table 2**

Values of pseudo-first order kinetic parameters and methyl orange dye decolorization for the low-temperature S-doped TiO<sub>2</sub> film along 12 photocatalytic cycles under visible light.

| Photocatalytic cycle | Initial $k_{app}$ constant (h <sup>-1</sup> ) | Last $k_{app}$ constant (h <sup>-1</sup> ) | R <sup>2</sup> | Dye decolorization (%) |
|----------------------|---|--|----------------|------------------------|
| 1st                  | $3.857 \times 10^{-4}$                        | $1.276 \times 10^{-3}$                     | 0.9984         | 72.1                   |
| 2nd                  | $3.826 \times 10^{-4}$                        | $1.248 \times 10^{-3}$                     | 0.9963         | 71.3                   |
| 3rd                  | $3.831 \times 10^{-4}$                        | $1.224 \times 10^{-3}$                     | 0.9835         | 70.6                   |
| 4th                  | $3.826 \times 10^{-4}$                        | $8.232 \times 10^{-4}$                     | 0.9918         | 56.1                   |
| 5th                  | $3.833 \times 10^{-4}$                        | $7.154 \times 10^{-4}$                     | 0.9189         | 51.1                   |
| 6th                  | $3.855 \times 10^{-4}$                        | $7.175 \times 10^{-4}$                     | 0.9523         | 51.2                   |
| 7th                  | $2.876 \times 10^{-4}$                        | $5.533 \times 10^{-4}$                     | 0.9726         | 42.5                   |
| 8th                  | $1.335 \times 10^{-4}$                        | $5.464 \times 10^{-4}$                     | 0.9795         | 42.1                   |
| 9th                  | $1.566 \times 10^{-4}$                        | $4.716 \times 10^{-4}$                     | 0.9882         | 37.6                   |
| 10th                 | $1.625 \times 10^{-4}$                        | $4.491 \times 10^{-4}$                     | 0.9708         | 36.2                   |
| 11th                 | $1.625 \times 10^{-4}$                        | $4.447 \times 10^{-4}$                     | 0.9646         | 35.9                   |
| 12th                 | $1.508 \times 10^{-4}$                        | $4.201 \times 10^{-4}$                     | 0.9653         | 34.3                   |

in the initial photoactivity value for  $2.9 \times 10^{-4} \text{ h}^{-1}$ , then to around  $k_{app} = 1.6 \times 10^{-4} \text{ h}^{-1}$ , which may be related to the dye impregnation on the catalyst surface, inhibiting its activity, as found by FTIR analysis. Increasing the concentration of dye impregnated on the catalyst surface may reduce the formation of electronic holes (h<sup>+</sup>) and HO• radicals on the surface, since the photoactive sites are blocked by the dye ions [43]. Furthermore, this action may promote a reduction of the dye removal kinetics, possibly due to the catalyst saturation by the dye [46]. The reduction in the  $k_{app}$  values indicates a lower dye removal rate, similar trend to that observed here after several photocatalytic cycles (Table 2).

Recent studies have been discussed the influence of the dye molecules on the photodegradation behavior of the catalysts [47–49]. The principal problems with the use of dyes in the photoactivity evaluation are the dye photosensitization of the catalyst surface, and the surface dye impregnation – similar trend observed in the present work. However, with the correct surface reusability method, the semiconductor photocatalysts can be reused longer time.

Methyl orange dye (C<sub>14</sub>H<sub>14</sub>N<sub>3</sub>SO<sub>3</sub>Na) is a compound formed by azo groups bonded to aromatic rings [1,50]. After 12 photocatalytic cycles under visible light, there was the dye impregnation on the S-TiO<sub>2</sub> films surface, and consequent formation of new compounds, as shown in Fig. 8a. The high resolution S2p XPS core-level spectrum after the experiments revealed that, in addition to the presence of SO<sub>4</sub><sup>2-</sup> surface groups at 168.9 eV – product of the sulfur doping process – the catalyst exhibited a binding energy component at 167.7 eV, corresponding to S<sup>4+</sup> [18,29]. The result corroborates the FTIR results, and the visible light photocatalytic process of dye decolorization, in which the sulfur in the +6 chemical state is reduced to +4 chemical state (Eqs. (4)–(6)). Furthermore, the presence of the S<sup>4+</sup> ion suggests the formation of SO<sub>3</sub><sup>2-</sup> groups on the TiO<sub>2</sub> films surface [15,51,52]. Two additional peaks were found at 164.7 eV and 163.6 eV, respectively, attributed to S<sup>2-</sup> anion

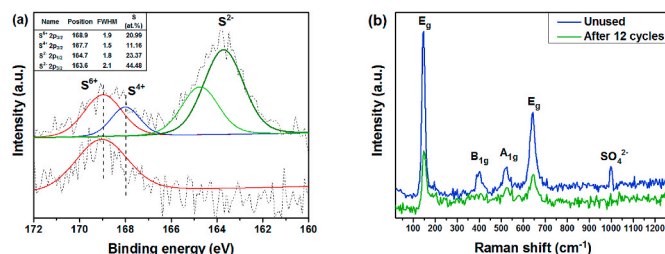


**Fig. 8.** (a) High resolution S2p XPS core-level spectra of the sulfur-doped TiO<sub>2</sub> film before and after 12 photocatalytic cycles for methyl orange dye decolorization under visible light; (b) Raman spectra of the S-TiO<sub>2</sub> photocatalyst before and after the recyclability experiments. (For interpretation of the references to color in this figure legend, the reader is referred to the Web version of this article.)

[30,51]. According to Hu et al. [53] and Augugliaro et al. [54] dyes formed by sulfur atoms can be reduced/oxidized to sulfate ions. TiO<sub>2</sub> films contain a high concentration of H–O groups on its surface [7,25]. During the photocatalytic process, H<sup>+</sup> is produced on the film surface (Eq. (1)). Thus, for acidic aqueous solutions, the Ti–OH bonds can be protonated, and produce a positive layer (Ti–OH<sub>2</sub><sup>+</sup>) on the surface [55], which can adsorb anionic methyl orange dye – effect that favors the dye impregnation of the catalyst surface, and the formation of Ti–OSO<sub>3</sub>H compounds.

Fig. 8b shows the Raman spectroscopy results for the sulfur-doped TiO<sub>2</sub> film before and after the photocatalytic experiments. The unused film presented peaks at 144 cm<sup>-1</sup>, 397 cm<sup>-1</sup>, 515 cm<sup>-1</sup>, and 639 cm<sup>-1</sup>, which are attributed, respectively, to the E<sub>g</sub>, B<sub>1g</sub>, A<sub>1g</sub>, and E<sub>g</sub> vibration modes of the TiO<sub>2</sub>-anatase phase [56,57]. No peaks related to the rutile phase or other TiO<sub>2</sub> polymorphs were observed [51]. The additional peak found at 981 cm<sup>-1</sup> corresponds to SO<sub>4</sub><sup>2-</sup> groups present on the TiO<sub>2</sub> films surface [58,59]. Peaks referring to TiS<sub>2</sub> or TiSx compounds were not found in Raman spectrum, which suggests their non-formation. A considerable change in the Raman profile was observed after using the S–TiO<sub>2</sub> film. The reduction in peak intensity may be associated with the impregnation of new ionic compounds on the S–TiO<sub>2</sub> film surface after use – similar trend obtained from the FTIR (Fig. 6) and XPS results (Fig. 8a). Such surface impregnation by the dye molecules, and the ionic compounds formed, can hinder the photon absorption on the catalyst surface [25,60], and promote the reduction of the S–TiO<sub>2</sub> photocatalytic activity over cycles – as noted in the recyclability experiments.

The use of ethanol for surface reusability of S-doped TiO<sub>2</sub> films performed well for a limited number of photocatalytic cycles. The obtained results support the possibility of reuse of films. Durability experiments have shown that the S-doped catalysts have good stability after several photocatalytic cycles, and that their reuse is possible over several cycles, which allows their practical environmental application with boa efficiency. The results suggest that TiO<sub>2</sub> films grown by MOCVD, and sulfur-doped at 50 °C is a facile route to produce promising catalysts for the dye decolorization water under sunlight by a green method.

## 4. Conclusions

This paper showed a preliminary performance evaluation about the possibility of surface reusability and photocatalytic reuse of TiO<sub>2</sub> films grown on borosilicate glass substrates at 400 °C by the MOCVD technique, and subsequently sulfur-doped at low temperature under a mixture of H<sub>2</sub>/H<sub>2</sub>S. The doping process was performed at 50 °C by a process similar to that used for the H<sub>2</sub>S desulfurization. The anatase-TiO<sub>2</sub> crystalline phase was identified in the films both before and after the 12-cycles dye degradation tests under visible light. The results demonstrated that the S-doped films have excellent photocatalytic activity, with an efficiency of 72.1% of the dye degradation in 5 h under visible light. Reuse experiments indicated that the catalysts have good photostability even after 16 h of use. From the 4th photocatalytic cycle there was a slight loss of photoactivity, until its stabilization in approximately 35%, which may be related to the effect of dye impregnation on the catalyst surface. Although there were no apparent morphological changes, a loss of wettability, and a change in the FTIR spectrum profile were observed, that suggests the impregnation of dye molecules on the catalyst surface. Such behavior suggests that the ethanol surface reusability method was not sufficient to completely eliminate adsorbed contaminants. However, the durability results support the possibility of S-doped catalyst reuse in water treatment and purification in a practical and efficient green method.

## CRedit authorship contribution statement

**Rodrigo T. Bento:** Conceptualization, Funding acquisition, Writing - original draft, substantial contribution to conception and design,

substantial contribution to acquisition of data, drafting the article. **Olandir V. Correia:** Conceptualization, Formal analysis, substantial contribution to conception and design, substantial contribution to analysis and interpretation of data. **Marina F. Pillis:** Conceptualization, substantial contribution to conception and design, critically revising the article for important intellectual content, final approval of the version to be published.

## Declaration of competing interest

The authors declare that they have no known competing financial interests or personal relationships that could have appeared to influence the work reported in this paper.

## Acknowledgments

The authors are grateful to CAPES, CNPq (Proc. 168935/2018–0), and FAPESP (Proc. 05/55861–4) Brazilian agencies for the financial support, UFABC (Federal University of ABC) for the XPS facility, and IQ-USP (Institute of Chemistry - University of São Paulo) for the contact angle measurements facility.

## References

- [1] R.T. Bento, M.F. Pillis, Titanium dioxide films for photocatalytic degradation of methyl orange dye, in: *Titanium Dioxide - Material for a Sustainable Environment*, InTech, London, 2018, pp. 211–226, <https://doi.org/10.5772/intechopen.75528>, 1ed.
- [2] O.A. Krysiak, P.J. Barczuk, K. Bienkowski, T. Wojciechowski, J. Augustynski, The photocatalytic activity of rutile and anatase TiO<sub>2</sub> electrodes modified with plasmonic metal nanoparticles followed by photoelectrochemical measurements, *Catal. Today* 321–322 (2019) 52–58, <https://doi.org/10.1016/j.cattod.2018.01.007>.
- [3] L. Lin, H. Wang, H. Luo, P. Xu, Enhanced photocatalysis using side-glowing optical fibers coated with Fe-doped TiO<sub>2</sub> nanocomposite thin films, *J. Photochem. Photobiol. Chem.* 307–308 (2015) 88–98, <https://doi.org/10.1016/j.jphotochem.2015.04.010>.
- [4] X. Zhang, M. Zhou, L. Lei, Preparation of an Ag–TiO<sub>2</sub> photocatalyst coated on activated carbon by MOCVD, *Mater. Chem. Phys.* 91 (2005) 73–79, <https://doi.org/10.1016/j.matchemphys.2004.10.058>.
- [5] M. Dhayal, R. Kapoor, P.G. Sistla, R.R. Pandey, S. Kar, K.K. Saini, G. Pande, Strategies to prepare TiO<sub>2</sub> thin films, doped with transition metal ions, that exhibit specific physicochemical properties to support osteoblast cell adhesion and proliferation, *Mater. Sci. Eng. C Mater. Biol. Appl.* 37 (2014) 99–107, <https://doi.org/10.1016/j.msec.2013.12.035>.
- [6] S. Krumdieck, R. Gorthy, J.G. Land, A.J. Gardecka, M.I.J. Polson, R. Boichot, C. M. Bishop, J.V. Kennedy, Titania solid thin films deposited by pp-MOCVD exhibiting visible light photocatalytic activity, *Phys. Status Solidi* 215 (2) (2018), <https://doi.org/10.1002/pssa.201870003>, 1870003.
- [7] R.T. Bento, O.V. Correia, M.F. Pillis, Photocatalytic activity of undoped and sulfur-doped TiO<sub>2</sub> films grown by MOCVD for water treatment under visible light, *J. Eur. Ceram. Soc.* 39 (2019) 3498–3504, <https://doi.org/10.1016/j.jeurceram Soc.2019.02.046>.
- [8] A.J. Gardecka, C. Bishop, D. Lee, S. Corby, I.P. Parkin, A. Kafizas, S. Krumdieck, High efficiency water splitting photoanodes composed of nanostructured anatase-rutile TiO<sub>2</sub> heterojunctions by pulsed-pressure MOCVD, *Appl. Catalysis B: Environ. Times* 224 (2018) 904–911, <https://doi.org/10.1016/j.apcatb.2017.11.033>.
- [9] Z. Wang, H.-H. Wu, Q. Li, F. Besenbacher, Y. Li, X.C. Zeng, M. Dong, Reversing interfacial catalysis of ambipolar WSe<sub>2</sub> single crystal, *Adv. Sci.* 7 (2020), <https://doi.org/10.1002/advs.201901382>, 1901382.
- [10] T. Guo, L. Wang, S. Sun, Y. Wang, X. Chen, K. Zhang, D. Zhang, Z. Xue, X. Zhou, Layered MoS<sub>2</sub>@graphene functionalized with nitrogen-doped graphene quantum dots as an enhanced electrochemical hydrogen evolution catalyst, *Chin. Chem. Lett.* 30 (2019) 1253–1260, <https://doi.org/10.1016/j.ccllet.2019.02.009>.
- [11] J. Feltrin, M.N. Sartor, A. De Noni Jr., A.M. Bernardin, D. Hotza, J.A. Labrincha, Photocatalytic surfaces of titania on ceramic substrates. Part I: synthesis, structure and photoactivity, *Cerâmica* 59 (2013) 620–632, <https://doi.org/10.1590/S0366-69132013000400020>.
- [12] M. Li, Z. Xing, J. Jiang, Z. Li, J. Kuang, J. Yin, N. Wan, Q. Zhu, W. Zhou, In-situ Ti<sup>3+</sup>/S doped high thermostable anatase TiO<sub>2</sub> nanorods as efficient visible-light-driven photocatalysts, *Mater. Chem. Phys.* 219 (2018) 303–310, <https://doi.org/10.1016/j.matchemphys.2018.08.051>.
- [13] R.T. Bento, A. Ferrus Filho, M.F. Pillis, Microstructural characterization of TiO<sub>2</sub> thin films: a review, *Revista Brasileira de Inovação Tecnológica em Saúde* 7 (2017) 4–17, <https://doi.org/10.18816/r-bits.v7i1>.
- [14] G.L.-M. Léonard, C.M. Malengreaux, Q. Mélotte, S.D. Lambert, E. Bruneel, I. V. Driessche, B. Heinrichs, Doped sol-gel films vs. powders TiO<sub>2</sub>: on the positive effect induced by the presence of a substrate, *J. Environ. Chem. Eng* 4 (1) (2016) 449–459, <https://doi.org/10.1016/j.jece.2015.11.040>.

- [15] C. Han, M. Pelaez, V. Likodimos, A.G. Kontos, P. Falaras, K. O'Shea, D. Dionysiou, Innovative visible light-activated sulfur doped TiO<sub>2</sub> films for water treatment, *Appl. Catalysis B: Environ. Times* 107 (2011) 77–87, <https://doi.org/10.1016/j.apcatb.2011.06.039>.
- [16] B. Anitha, C. Ravidhas, R. Venkatesh, A.M.E. Raj, K. Ravichandran, B. Subramanian, C. Sanjeeviraja, Self assembled sulfur induced interconnected nanostructure TiO<sub>2</sub> electrode for visible light photoresponse and photocatalytic application, *Physica E. Low Dimens. Syst. Nanostruct* 91 (2017) 148–160, <https://doi.org/10.1016/j.physe.2017.04.017>.
- [17] X. Yan, K. Yuan, N. Lu, H. Xu, S. Zhang, N. Takeuchi, H. Kobayashi, R. Li, The interplay of sulfur doping and surface hydroxyl in band gap engineering: mesoporous sulfur-doped TiO<sub>2</sub> coupled with magnetite as a recyclable, efficient, visible light active photocatalyst for water purification, *Appl. Catalysis B: Environ. Times* 218 (2017) 20–31, <https://doi.org/10.1016/j.apcatb.2017.06.022>.
- [18] T. Ohno, M. Akiyoshi, T. Umebayashi, K. Asai, T. Mitsui, M. Matsumura, Preparation of S-doped TiO<sub>2</sub> photocatalysts and their photocatalytic activities under visible light, *Appl. Catalysis A-General* 265 (2004) 115–121, <https://doi.org/10.1016/j.apcata.2004.01.007>.
- [19] M.R. Bayati, A.Z. Moshfegh, F. Golestani-Fard, On the photocatalytic activity of the sulfur doped titania nano-porous films derived via micro-arc oxidation, *Appl. Catalysis. A, GEN* 389 (2010) 60–67, <https://doi.org/10.1016/j.apcata.2010.09.003>.
- [20] M.C. Canela, R.M. Alberici, W.F. Jardim, Gas-phase destruction of H<sub>2</sub>S using TiO<sub>2</sub>/UV-VIS, *J. Photochem. Photobiol. Chem.* 112 (1998) 73–80, [https://doi.org/10.1016/S1010-6030\(97\)00261-X](https://doi.org/10.1016/S1010-6030(97)00261-X).
- [21] M.F. Pillis, O.V. Correa, R.T. Bento, Brazilian patent No. BR1020190112182, Retrieved from, <https://gru.inpi.gov.br/pepi/servlet/PatenteServletController?Action=detail&CodPedido=1512369&SearchParameter=BR%20102019011218-2%20%20%20%20%20%20%20&Resumo=&Titulo=>, 2019.
- [22] B.A. Marcello, O.V. Correa, R.T. Bento, M.F. Pillis, Effect of growth parameters on the photocatalytic performance of TiO<sub>2</sub> films prepared by MOCVD, *J. Braz. Chem. Soc.* 31 (2020) 1270–1283, <https://doi.org/10.21577/0103-5053.202000012>.
- [23] F. Zhang, M. Wang, X. Zhu, B. Hong, W. Wang, Z. Qi, W. Xie, J. Ding, J. Bao, S. Sun, C. Gao, Effect of surface modification with H<sub>2</sub>S and NH<sub>3</sub> on TiO<sub>2</sub> for adsorption and photocatalytic degradation of gaseous toluene, *Appl. Catal. B Environ.* 170–171 (2015) 215–224, <https://doi.org/10.1016/j.apcatb.2015.01.045>.
- [24] Y.-H. Lin, H.-T. Hsueh, C.-W. Chang, H. Chu, The visible light-driven photodegradation of dimethyl sulfide on S-doped TiO<sub>2</sub>: characterization, kinetics, and reaction pathways, *Appl. Catal. B Environ.* 199 (2016) 1–10, <https://doi.org/10.1016/j.apcatb.2016.06.024>.
- [25] E.C. de Oliveira, R.T. Bento, O.V. Correa, M.F. Pillis, Visible-light photocatalytic activity and recyclability of N-doped TiO<sub>2</sub> films grown by MOCVD, *Cerâmica* 66 (380) (2020) 451–459, <https://doi.org/10.1590/0366-69132020663802957>.
- [26] L. Pan, J.-J. Zou, S. Wang, Z.-F. Huang, X. Zhang, L. Wang, Enhancement of visible-light-induced photodegradation over hierarchical porous TiO<sub>2</sub> by nonmetal doping and water-mediated dye sensitization, *Appl. Surf. Sci.* 268 (2013) 252–258, <https://doi.org/10.1016/j.apsusc.2012.12.074>.
- [27] E.A. Souza Filho, E.F. Pieretti, R.T. Bento, M.F. Pillis, Effect of nitrogen-doping on the surface chemistry and corrosion stability of TiO<sub>2</sub> films, *J. Mater. Res. Technol* 9 (2020) 922–934, <https://doi.org/10.1016/j.jmrt.2019.11.032>.
- [28] R. Portela, B. Sánchez, J.M. Coronado, Photocatalytic oxidation of H<sub>2</sub>S on TiO<sub>2</sub> and TiO<sub>2</sub>-ZrO<sub>2</sub> thin films, *J. Adv. Oxid. Technol.* 10 (2) (2007) 375–380, <https://doi.org/10.1515/jaots-2007-0223>.
- [29] T. Ohno, N. Murakami, Development of visible-light active S cation-doped TiO<sub>2</sub> photocatalyst, *Curr. Org. Chem.* 14 (7) (2010) 699–708, <https://doi.org/10.2174/1385527210790963386>.
- [30] T. Umebayashi, T. Yamaki, H. Itoh, K. Asai, Band gap narrowing of titanium dioxide by sulfur doping, *Appl. Phys. Lett.* 81 (3) (2002) 454–456, <https://doi.org/10.1063/1.1493647>.
- [31] L.G. Devi, R. Kavitha, Enhanced photocatalytic activity of sulfur doped TiO<sub>2</sub> for the decomposition of phenol: a new insight into the bulk and surface modification, *Mater. Chem. Phys.* 143 (2014) 1300–1309, <https://doi.org/10.1016/j.matchemphys.2013.11.038>.
- [32] Y.-H. Lin, S.-H. Chou, H. Chu, A kinetic study for the degradation of 1,2-dichloroethane by S-doped TiO<sub>2</sub> under visible light, *J. Nanoparticle Res.* 16 (8) (2014) 1–12, <https://doi.org/10.1007/s11051-014-2539-3>.
- [33] N. Shatohri, D. Sud, A greener approach to synthesize visible light responsive nanoporous S-doped TiO<sub>2</sub> with enhanced photocatalytic activity, *New J. Chem.* 39 (3) (2015) 2217–2223, <https://doi.org/10.1039/C4NJ01422G>.
- [34] Y. Chen, Y. Jiang, W. Li, R. Jin, S. Tang, W. Hu, Adsorption and interaction of H<sub>2</sub>S/SO<sub>2</sub> on TiO<sub>2</sub>, *Catal. Today* 50 (1999) 39–47, [https://doi.org/10.1016/S0920-5861\(98\)00460-X](https://doi.org/10.1016/S0920-5861(98)00460-X).
- [35] O. Carp, C.L. Huisman, A. Reller, Photoinduced reactivity of titanium dioxide, *Prog. Solid State Chem.* 32 (2004) 33–177, <https://doi.org/10.1016/j.progsolidstchem.2004.08.001>.
- [36] Y. Xiong, D. He, R. Jaber, P.J. Cameron, K.J. Edler, Sulfur-doped cubic mesostructured titania films for use as a solar photocatalyst, *J. Phys. Chem. C* 121 (18) (2017) 9929–9937, <https://doi.org/10.1021/acs.jpcc.7b01615>.
- [37] G. Yang, Z. Yan, T. Xiao, Low-temperature solvothermal synthesis of visible-light-responsive S-doped TiO<sub>2</sub> nanocrystal, *Appl. Surf. Sci.* 258 (2012) 4016–4022, <https://doi.org/10.1016/j.apsusc.2011.12.092>.
- [38] T. Shen, C. Jiang, C. Wang, J. Sun, X. Wang, X. Li, A TiO<sub>2</sub> modified abiotic–biotic process for the degradation of the azo dye methyl orange, *RSC Adv.* 5 (72) (2015) 58704–58712, <https://doi.org/10.1039/C5RA06686G>.
- [39] Q. Jiahao, Y. Feng, X. Zhang, J. Mingmin, J. Fao, Acid-promoted synthesis of UiO-66 for highly selective adsorption of anionic dyes: adsorption performance and mechanisms, *J. Colloid Interface Sci.* 499 (2017) 151–158, <https://doi.org/10.1016/j.jcis.2017.03.101>.
- [40] D. Duc La, A. Rananaware, H.P. NguyenThi, L. Jones, S.V. Bhosale, Fabrication of a TiO<sub>2</sub>@porphyrin nanofiber hybrid material: a highly efficient photocatalyst under simulated sunlight irradiation, *Adv. Nat. Sci. Nanosci. Nanotechnol.* 8 (2017), <https://doi.org/10.1088/2043-6254/aa597e>, 015009.
- [41] K. Kato, S. Vaucher, P. Hoffmann, Y. Zin, T. Shirai, A novel single-mode microwave assisted synthesis of metal oxide as visible-light photocatalyst, *Mater. Letters* 235 (2019) 125–128, <https://doi.org/10.1016/j.matlet.2018.09.132>.
- [42] C.W. Dunnill, Z.A. Aiken, A. Kafizas, J. Pratten, M. Wilson, D.J. Morgan, I. P. Parkin, White light induced photocatalytic activity of sulfur-doped TiO<sub>2</sub> thin films and their potential for antibacterial application, *J. Mater. Chem.* 19 (2009) 8747–8754, <https://doi.org/10.1039/B913793A>.
- [43] N. Guettaï, H.A. Amar, Photocatalytic oxidation of methyl orange in presence of titanium dioxide in aqueous suspension, Part II: kinetics study, *Desalination* 185 (1–3) (2005) 439–448, <https://doi.org/10.1016/j.desal.2005.04.049>.
- [44] Y. He, F. Grieser, M. Ashokkumar, The mechanism of sonophotocatalytic degradation of methyl orange and its products in aqueous solutions, *Ultrason. Sonochem.* 18 (5) (2011) 974–980, <https://doi.org/10.1016/j.ultrsonch.2011.03.017>.
- [45] F. Wang, F. Li, L. Zhang, H. Zeng, Y. Sun, S. Zhang, X. Xu, S-TiO<sub>2</sub> with enhanced visible-light photocatalytic activity derived from TiS<sub>2</sub> in deionized water, *Mater. Res. Bull.* 87 (2017) 20–26, <https://doi.org/10.1016/j.materresbull.2016.11.014>.
- [46] S.A. Qaradawi, S.R. Salman, Photocatalytic degradation of methyl orange as a model compound, *J. Photochem. Photobiol. Chem.* 148 (2002) 161–168, [https://doi.org/10.1016/S1010-6030\(02\)00086-2](https://doi.org/10.1016/S1010-6030(02)00086-2).
- [47] N. Shaham-Waldmann, Y. Paz, Away from TiO<sub>2</sub>: a critical minireview on the developing of new photocatalysts for degradation of contaminants in water, *Mater. Sci. Semicond. Process.* 42 (2016) 72–80, <https://doi.org/10.1016/j.msspp.2015.06.068>.
- [48] M. Rochkind, S. Pasternak, Y. Paz, Using dyes for evaluating photocatalytic properties: a critical review, *Molecules* 20 (2014) 88–110, <https://doi.org/10.3390/molecules20010088>.
- [49] S. Bae, S. Kim, S. Lee, W. Choi, Dye decolorization test for the activity assessment of visible light photocatalysts: realities and limitations, *Catal. Today* 224 (2014) 21–28, <https://doi.org/10.1016/j.cattod.2013.12.019>.
- [50] Y. Sha, I. Mathew, Q. Cui, M. Clay, F. Gao, X.J. Zhang, Z. Gu, Rapid degradation of azo dye methyl orange using hollow cobalt nanoparticles, *Chemosphere* 144 (2016) 1530–1535, <https://doi.org/10.1016/j.chemosphere.2015.10.040>.
- [51] S.A. Etghani, E. Ansari, S. Mohajezadeh, Evolution of large area TiS<sub>2</sub>-TiO<sub>2</sub> heterostructures and S-doped TiO<sub>2</sub> nano-sheets on titanium foils, *Sci. Rep.* 9 (2019), <https://doi.org/10.1038/s41598-019-53651-y>, 17943.
- [52] Z. Wang, P. Li, Y. Chen, J. He, W. Zhang, O.G. Schmidt, Y. Li, Pure thiophene-sulfur doped reduced graphene oxide: synthesis, structure, and electrical properties, *Nanoscale* 6 (2014) 7281–7287, <https://doi.org/10.1039/C3NR05061K>.
- [53] C. Hu, J.C. Yu, Z. Hao, P.K. Wong, Photocatalytic degradation of triazine-containing azo dyes in aqueous TiO<sub>2</sub> suspensions, *Appl. Catal., B* 42 (2003) 47–55, [https://doi.org/10.1016/S0926-3373\(02\)00214-X](https://doi.org/10.1016/S0926-3373(02)00214-X).
- [54] V. Augugliaro, C. Baiocchi, A. Bianco Prevot, E. García-López, V. Lodo, S. Malato, G. Marci, L. Palmisano, M. Pazzi, E. Pramauro, Azo-dyes photocatalytic degradation in aqueous suspension of TiO<sub>2</sub> under solar irradiation, *Chemosphere* 49 (2002) 1223–1230, [https://doi.org/10.1016/S0045-6535\(02\)00489-7](https://doi.org/10.1016/S0045-6535(02)00489-7).
- [55] H.C. Liang, X.Z. Li, J. Nowotny, Photocatalytic properties of TiO<sub>2</sub> nanotubes, *Solid State Phenom.* 162 (2010) 295–328, <https://doi.org/10.4028/www.scientific.net/SSP.162.295>.
- [56] N. Li, X. Zhang, W. Zhou, Z. Liu, G. Xie, Y. Wang, Y. Du, High quality sulfur-doped titanium dioxide nanocatalysts with visible light photocatalytic activity from non-hydrolytic thermolysis synthesis, *Inorg. Chem. Front* 1 (2014) 521–525, <https://doi.org/10.1039/C4QI00027G>.
- [57] I.I. Kabir, L.R. Sheppard, R. Shamiri, P. Koshy, R. Liu, W. Joe, A. Le, X. Lu, W. F. Chen, C.C. Sorrell, Contamination of TiO<sub>2</sub> thin films spin coated on borosilicate and rutile substrates, *J. Mater. Sci.* 55 (2020) 3774–3794, <https://doi.org/10.1007/s10853-019-04282-1>.
- [58] M.D. Fontana, K.B. Mabrouk, T.H. Kauffmann, Raman spectroscopic sensors for inorganic salts, in: *Spectroscopic Properties of Inorganic and Organometallic Compounds: Techniques, Materials and Applications*, vol. 44, RSC Publishing, London, 2013, pp. 40–67, <https://doi.org/10.1039/9781849737791-00040>.
- [59] I. Giakoumelou, V. Parvulescu, S. Boghosian, Oxidation of sulfur dioxide over supported solid V<sub>2</sub>O<sub>5</sub>/SiO<sub>2</sub> and supported molten salt V<sub>2</sub>O<sub>5</sub>-Cs<sub>2</sub>SO<sub>4</sub>/SiO<sub>2</sub> catalysts: molecular structure and reactivity, *J. Catal.* 225 (2004) 337–349, <https://doi.org/10.1016/j.jcat.2004.04.012>.
- [60] S. Bae, S. Kim, S. Lee, W. Choi, Dye decolorization test for the activity assessment of visible light photocatalysts: realities and limitations, *Catal. Today* 224 (2014) 21–28, <https://doi.org/10.1016/j.cattod.2013.12.019>.